Colloids and Surfaces B: Biointerfaces 189 (2020) 110851

Contents lists available at ScienceDirect

Colloids and Surfaces B: Biointerfaces

journal homepage: www.elsevier.com/locate/colsurfb

Silicon-hydroxyapatite–glycerohydrogel as a promising biomaterial for dental applications

T.G. Khonina[a,*], O.N. Chupakhin[a,b], V.Ya. Shur[c], A.P. Turygin[c], V.V. Sadovsky[d], Yu.V. Mandra[d], E.A. Sementsova[d], A.Yu Kotikova[d], A.V. Legkikh[d], E.Yu Nikitina[a], E.A. Bogdanova[e], N.A. Sabirzyanov[e]

[a] Postovsky Institute of Organic Synthesis, Ural Branch, Russian Academy of Sciences, 620990, Ekaterinburg, Russia
[b] Institute of Chemical Engineering, Ural Federal University, 620002, Ekaterinburg, Russia
[c] Institute of Natural Sciences and Mathematics, Ural Federal University, 620000, Ekaterinburg, Russia
[d] Ural State Medical University, 620219, Ekaterinburg, Russia
[e] Institute of Solid State Chemistry, Ural Branch, Russian Academy of Sciences, 620990, Ekaterinburg, Russia

ARTICLE INFO

Keywords:
Silicon-hydroxyapatite–glycerohydrogel
Structure
Tooth enamel
Remineralization
Surface roughness
Microhardness

ABSTRACT

Nanocomposite silicon-hydroxyapatite–glycerohydrogel (Si-HA–glycerohydrogel) with different hydroxyapatite (HA) contents of 0.75 and 1.75 wt.% and the same Si content (2.04 wt.%) was obtained by the sol–gel method. Silicon tetraglycerolate in the form of glycerol solution was used as a biocompatible precursor and HA in the form of aqueous colloidal suspension – as a template and property modifier. Transmission electron microscopy was applied to demonstrate that there are nanoscale HA particles that are in the crystalline state. For the first time, using the atomic force microscopy method, the remineralizing properties of Si-HA–glycerohydrogel were studied on human teeth extracted for orthodontic reasons. It was found that Si-HA–glycerohydrogel containing 1.75 wt.% HA has a pronounced remineralizing effect. Immersion of tooth enamel samples in the gel for one month significantly reduces roughness and makes the enamel surface more uniform. Silicon contained in glycerolates in a biologically active and accessible form exerts an additional positive effect on the process of remineralization of tooth enamel. By the energy dispersive X-ray analysis, it was demonstrated that the tooth enamel had an increased silicon content; and the Vickers microhardness test showed greater microhardness values. The obtained data analysis allows the remineralizing Si-HA–glycerohydrogel to be considered as a promising biomaterial for dental applications.

1. Introduction

Sol–gel synthesis is widely used for producing materials with a complex of useful properties, which make them promising materials for biomedical applications [1–5]. The use of polyolate precursors is known to be preferable in such sol–gel processes, for example, silicon polyolates can be applied, which are water soluble derivatives of polyatomic alcohols [6–10]. When commonly used alkoxy precursors, such as tetraethoxysilane $Si(OEt)_4$, are involved in the sol–gel process, monoatomic alcohol is released, which may result in denaturation and/or precipitation of biomacromolecules. Unlike monoatomic alcohols, polyols have no negative effect on the biomacromolecules. Moreover, the sol–gel process proceeds under mild conditions without using additional homogenizing solvent or catalyst.

We have earlier developed a design strategy for the sol–gel synthesis of hydrogels containing biogenic elements to be useful in medical applications. The essence of the strategy is that polyolates of biogenic elements, mainly silicon glycerolates, are used as biocompatible precursors in sol–gel processing, as a rule, in the form of the solution of the corresponding polyol approved for a certain medical application. Thus combined polyolates are used to achieve a synergistic pharmacological effect; and bioactive additives or drugs serve as templates and/or as property modifiers for the formed hydrogel [9,10].

Based on the strategy, we have synthesized by sol–gel method a bioactive silicon-hydroxyapatite–glycerohydrogel (Si-HA–glycerohydrogel) [11] from the glycerol solution of silicon tetraglycerolate $Si(C_3H_7O_3)_4$ (silicon glycerolates) [12] and an aqueous colloidal suspension of hydroxyapatite (HA) [13].

Silicon glycerolates were synthesized by alcoholysis of $Si(OEt)_4$ with glycerol excess. Silicon glycerolates are observed as an equilibrium mixture of $Si(C_3H_7O_3)_4$ and low-molecular products of intermolecular condensation, with the glycerol excess hindering the formation of

* Corresponding author.
E-mail address: khonina@ios.uran.ru (T.G. Khonina).

https://doi.org/10.1016/j.colsurfb.2020.110851
Received 7 November 2019; Received in revised form 5 February 2020; Accepted 6 February 2020
Available online 07 February 2020
0927-7765/

condensation products [9]. Silicon glycerolates and hydrogels based thereof are non-toxic, safe in application and exhibit pronounced wound-healing and percutaneous activity [12]. Because of their high penetrating activity, they promote penetration of drugs or bioactive additives into injured tissues. Silicon contained in glycerolates in a biologically active and accessible form has a stimulating effect on all kinds of tissues (epithelial, fibrous, bone), accelerating the reparation and regeneration processes [14].

HA is the main inorganic compound constituting the natural bone, tooth enamel and dentin; HA has a hexagonal crystal structure and is described with a chemical formula $Ca_{10}(PO_4)_6(OH)_2$ [15–17]. Thanks to its superior biocompatibility and excellent bioactivity characteristics, HA is known to have been used in many fields of clinical medicine as a solution designed to assist in correcting regeneration problems in soft and bone tissues [16,18–20]. The biological activity of HA depends considerably on its particle size. The higher is the HA dispersion, the greater is the biological activity of the substance [21].

HA nanoparticles are produced using various methods such as mechanochemical synthesis, combustion preparation and various wet chemistry techniques [16,22–24] and as a result, HA nanoparticles come in variety of shapes, atomic arrangements and orientations [25]. The resulted particles can be used as high-performance biomaterial capable of adsorbing bio-related substances, and can also be utilized as a model system for tooth enamel [21,25]. Therefore, HA shows promise as a material to be used in the remineralizing systems applied to tooth enamel [20,21,26–30], particularly, in toothpastes [31,32].

The obtained Si-HA–glycerohydrogel [11] combines useful pharmacological properties characteristic of both silicon glycerolates and HA. The gel causes a reparative, regenerative and osteoplastic effect [33] and can be used for curing wounds of different etiology and for treating periodontal tissues.

It seems logical to assume that the use of Si-HA–glycerohydrogel for the treatment of periodontal disease can provide an additional remineralizing effect on tooth enamel, removing (smoothing) microdamages, and thereby restoring and strengthening it. In this case, silicon in a biologically active and accessible form could cause an additional positive effect on the process of remineralization of tooth enamel. However, this assumption was not experimentally proved.

It should be noted that literature seems to have little or scarce publications concerning the effect of bioactive silicon on tooth enamel. It was shown that the silicon incorporation might have certain biological significance, because silicon, along with calcium, phosphorus, and fluorine induces remineralization of demineralized tooth enamel and dentine *in vitro* [34–38]. Bioactive silicon is also known to cause proliferation of osteoblasts and to increase production of collagen in human bodies [14].

Thus, the purpose of this work was to study the remineralizing properties *(in vitro)* of Si-HA–glycerohydrogel.

2. Materials and methods

2.1. Materials

Tetraethoxysilane or $Si(OC_2H_5)_4$ (reagent grade, Russia) and glycerol or $C_3H_8O_3$ (analytical grade, Russia) were distilled at atmospheric pressure and *in vacuo*, respectively. Calcium hydroxide $Ca(OH)_2$ (analytical grade, Russia) and phosphoric acid H_3PO_4 (analytical grade, Russia) were used as received.

2.1.1. Synthesis of silicon glycerolates in 6 M excess of glycerol

The synthesis of silicon glycerolates with 6 M excess of $C_3H_8O_3$ was carried out according to ref. [12] by alcoholysis of $Si(OC_2H_5)_4$ with an excess of $C_3H_8O_3$ at a molar ratio of 1 : 10 and by heating up to 130 °C during 3 h, followed by the removal of ethanol under atmospheric pressure and then *in vacuo* by means of a rotary evaporator carried out to a constant weight (which corresponds to the theoretical loss of alcohol). The reaction completion was controlled by ^{1}H NMR (Fig. S1) by the absence of signals from residual ethoxy group protons at the silicon atom in the δH range 1.08–1.18 ppm (*t*, 3 H, Me). The product obtained is a colorless transparent viscous liquid readily soluble in water. Its composition corresponds to a $Si(C_3H_7O_3)_4$ – $C_3H_8O_3$ molar ratio 1 : 6. The elemental analysis and IR spectroscopy (Fig. S2a) confirm the resulted data [9,12].

2.1.2. The synthesis of HA aqueous colloidal suspension

The synthesis of a HA aqueous colloidal suspension was carried out according to ref. [13] by mixing the $Ca(OH)_2$ 0.02 M aqueous solution saturated at room temperature and 0.7 M H_3PO_4 solution at a volume ratio of components (3.75 ÷ 5.00) : 1 by the equation:

$$10Ca(OH)_2 + 6H_3PO_4 \rightarrow Ca_{10}(PO_4)_6(OH)_2 + 18H_2O.$$

The initial mixture was stirred at room temperature for 15 min. As a result of the interaction of initial substances taken in the proposed quantitative ratio, a HA aqueous colloidal suspension is formed, which typically represents a heterogeneous, highly dispersive system. The clarified upper layer formed during storage of a HA aqueous colloidal suspension was consistently drained to a HA content of 2.40 wt.%. The HA aggregates are characterized by a low positive value of ξ-potential (about +5 mV) that cannot provide stability of the system, so the HA is characterized with significant aggregative instability and segregation during storage. The particle size measurements showed that the system appears to be polydisperse with an average aggregative particle size of ~3.6 μm.

Then HA aqueous colloidal suspension (2.40 wt.%) was brought to a content of 5.68 wt.%. The value of ξ-potential was about +3 mV. The small value also indicates that the system is unstable. This is also a polydisperse system with an average aggregative particle size of ~4.3 μm.

Crystalline HA of the composition $Ca_{10}(PO_4)_6(OH)_2$ is formed in the process of drying. The X-ray diffraction pattern of the resulting compound (Fig. S3) is identical to that of synthetic HA (JCPDSD-ICDD, card number 09–432).

2.1.3. The synthesis of Si-HA–glycerohydrogel 1 (gel 1)

Si-HA–glycerohydrogel 1 (gel 1) was prepared at room temperature according to ref. [11] from a silicon glycerolates solution in glycerol (at a $Si(C_3H_7O_3)_4$ – $C_3H_8O_3$ molar ratio of 1 : 6) [12] and HA aqueous colloidal suspension (2.40 wt.%) [13] at a mass ratio of 2.19 : 1.00. The HA content in the resulting gel was 0.75 wt.%. The results of elemental analysis and IR spectroscopy matched the data in ref. [11]. Experimental (%): Si, 2.10; Ca, 0.27; P, 0.11. Calculated (%): Si, 2.04; Ca, 0.30; P, 0.14.

2.1.4. The synthesis of Si-HA–glycerohydrogel 2 (gel 2)

Si-HA–glycerohydrogel 2 (gel 2) was prepared similarly to gel 1 at room temperature from a silicon glycerolates solution in glycerol (at a Si $(C_3H_7O_3)_4$ – $C_3H_8O_3$ molar ratio of 1 : 6) [12] and HA aqueous colloidal suspension (5.68 wt.%) at a mass ratio of 2.19 : 1.00. The HA content in the resulting gel was 1.75 wt.%. Experimental (%): Si, 2.13; Ca, 0.65; P, 0.27. Calculated (%): Si, 2.04; Ca, 0.71; P, 0.33. IR spectrum (Fig. S4), ν/cm^{-1}: 3400 (O–H), 2932, 2883 (C–H), 1210 (CH_2), 1640 (H–O–H), 1110 (C–O in C–O–H secondary), 1040 (C–O in C–O–H primary), 1110, 1040, 990 (Si–O–C, P–O in PO_4^{3-}), 670, 560 (O–H, P–O in PO_4^{3-}).

2.1.5. The synthesis of model system

Model system was prepared from $C_3H_8O_3$ and HA aqueous colloidal suspension (5.68 wt.%) at a mass ratio of 2.19 : 1.00. The HA content in the resulting model system was 1.75 wt.%, which corresponded to the HA content in gel 2.

2.1.6. Preparation of tooth enamel microsections

The remineralizing effect was studied on enamel microsections taken from human teeth. The teeth were extracted for orthodontic

reasons from patients aged 18–30 years. The microsections were obtained by cutting a tooth crown with a diamond tool during water-cooling. The lateral areas of the microsections were finished by polishing discs of decreasing abrasiveness.

The resulted plates were 2 mm thick, 4 mm wide and 5 mm in height.

For the Vickers microhardness test, the samples were polished successively with silicon carbide papers No. 1200 to 4000 in water. Final polish was done with 0.05 polishing alumina in a low-speed metallurgical polisher with a light load on the sample. Upon polishing, the samples were cleaned with distilled water inside an ultrasonic cleaner during three 5 min periods.

2.1.7. Investigation of remineralizing properties

To study remineralizing properties of gels 1 and 2 by AFM, six tooth enamel samples were used, with three samples used for each gel. The tooth enamel samples were examined before and after a one-month immersion in a microtubes with 6 mL of gels 1 and 2 at room temperature.

For energy dispersive X-ray analysis, 15 tooth enamel samples were used, with the microsections of $2 \times 4 \times 5\,mm^3$ in size. Five of the samples were cut in half, and one half of each of the samples was immersed in gel 2, with the other half immersed in the model system. The remaining ten samples were used as control samples (without treatment).

Besides, the same samples immersed in gel 2 and model system, were investigated by the Vickers microhardness test.

2.2. Methods

Elemental analysis (C, H) was carried out using a Perkin Elmer PE 2400 elemental analyzer (series II CHNS–O EA 1108). IR spectra were recorded on a Nicolet 6700 Thermo Scientific spectrometer at 400–4000 cm^{-1}. Atomic emission spectrometry (Si, Ca, P) was performed using an iCAP 6300 Duo Thermo Scientific optical emission spectrometer. X-Ray diffraction analysis was carried out using a Shimadzu XRD 700 X-ray diffractometer (Cu K_α radiation).

Transmission electron microscope (TEM) observation was performed with samples prepared by drying a puttied drop of a HA aqueous colloidal suspension and an ultrasonically dispersed piece of Si-HA–glycerohydrogel in ethanol on a copper grid *in vacuo* at room temperature. A micrograph was taken on a Jeol Jem 2100 high-resolution transmission electron microscope with an Olympus Cantaga G2 digital camera and an Oxford Inca EnergyTEM 250 unit for microanalysis at the acceleration voltage of 200 kV and amperage of 105 mA.

The quantity of Si, Ca, and P were observed using a Quanta 200 FEI SEM with a Pegasus elemental analysis (energy dispersive X-ray analysis) system operating at 300 kV with spatial resolution about 5 nm.

Electrokinetic potential ζ (zeta-potential) measurements were carried out on a Brookhaven Zeta Plus universal analyzer using the electrophoretic light scattering method based on the measurement of Doppler shift of the frequency of light scattered by particles moving in DC electric field [39]. Particle size measurements were carried out in colloidal suspensions using the same analyzer following the dynamic light scattering method [40]. In light scattering measurements, initial precursor solutions were diluted down to 0.1 %. PS latex PSL with a particle size of 40 nm and zeta-potential standard BI-ZR3 (−53 mV) were used as standard samples. The standard deviation from manufacturer values did not increase more than by 2 %. All the measurements were carried out at 25 °C.

Atomic force microscopy (AFM) observation was carried out with a scanning probe microscope MFP-3D (Asylum Research, USA) and Probe Nanolaboratory NTEGRA Therma (NT-MDT, Russia) in tapping mode using DPE15 Ti/Pt probes (MikroMash, Estonia) having a radius of curvature about 30 nm, a resonant frequency of 325 kHz and with the spring constant at 40 N/m. Digital processing and data analysis were performed with IgorPro (Asylum Research, USA) and SPIP (SPIP, Denmark).

The Vickers microhardness measurements were carried out with a PMT 3 microhardness tester (Russia) with a square based diamond indenter with 136° angle, using a load of 200 g with a dwell time of 15 s. To measure the Vickers hardness number (VHN), ten Vickers tests were performed on each sample surface, and the mean value was calculated and determined as VHN (MPa). Distances between indentation points and disc borders were above 1 mm. Student's *t*-test was used to compare the mean surface microhardness values with a level of significance set at $p < 0.05$. The mean (± SD) values and relative changes in the surface microhardness values were calculated.

3. Results and discussion

Si-HA–glycerohydrogel (gel 1) containing 0.75 wt.% of HA and 2.04 wt.% of Si was obtained earlier [11] as a result of interaction between glycerol solution of silicon glycerolates (at a $Si(C_3H_7O_3)_4 – C_3H_8O_3$ molar ratio of 1 : 6) with aqueous colloid suspension of HA (2.40 wt.%). Using SEM method, it was demonstrated that HA, acting as a template promotes ordering of the gel structure [11] (Fig. S5). A number of advanced physical methods have also been utilized to demonstrate that the formed 3D-network of the Si-HA–glycerohydrogel contains Si–O–Si fragments and residual glyceroxy groups bonded to the silicon atoms (Fig. S2b). The residual glyceroxy groups are present in the network because there is an excess of glycerol in the system and hydrolysis of silicon glycerolates in the sol–gel processing is incomplete [9,12]. The cells of the network have been shown to be occupied by HA not covalently bound to the network, and HA has been identified in the crystalline form, according to the X-ray diffraction data, in solid phase extracted from the gel [11] (Fig. S6).

In this paper, the structural features of Si-HA–glycerohydrogel were studied by the TEM method. Fig. 1 shows the TEM micrographs of the samples obtained by drying a suspension of gel 1 in ethanol (Fig. 1.1) and a puttied drop of HA aqueous colloidal suspension (Fig. 1.2) on a copper grid.

The data obtained for gel 1 (Fig. 1.1) reveal the point and ring reflections in the electron diffraction area (a), which correspond to a crystalline substance, in this case, HA. Besides, the data confirm the nanoscale of the particles in the high-resolution area (b). It was shown that nanoscale HA particles in the dried colloidal suspension are in the crystalline state (Fig. 1.2).

Because HA is crystallochemically similar to tooth enamel and is highly biocompatible, nanoscale HA appears to be an ideal material for restoration of damaged teeth [21,26–30]. It is known that the tooth enamel's packing order ranges from the nanoscale of long calcium hydroxyapatite crystals to the microscale crystals aligned together in bundles forming prisms or rods with diameter from 3 to 5 μm. It is known that the basic building blocks of enamel represent 20–40 nm HA nanoparticles, and the enamel repairing effect of HA can be improved considerably if its dimensions are reduced to the same sizes [28].

In recent years, a great deal of interest has been focused on the development of AFM method, which is a valuable tool for analysis in relation to biomedical application [41,42]. In particular AFM was used for measuring the tooth enamel roughness while investigating demineralization and remineralization processes [43–46]. As for now, however, there seems to have been no comprehensible criteria developed for the morphometric analysis, which would allow a reliable comparison to be made for AFM images of tooth enamel samples. Using AFM, we estimated the variation in the surface roughness of enamel microsections before and after a one-month immersion in the gels studied at room temperature.

Fig. 2 shows the typical for AFM topography (a, b) and 3D-image (c, d) of the tooth enamel surface before and after immersion in gel 1 by example of sample 1 (see Table 1).

For quantitative characterization of enamel surface relief, the surface topography was measured. The values of arithmetical mean (S_a)

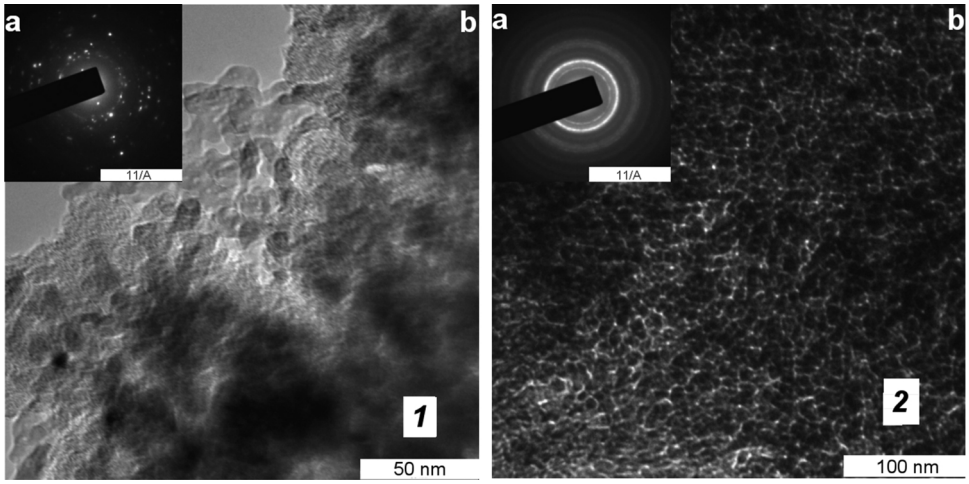

Fig. 1. TEM micrographs of (1) dried suspension of gel 1 in ethanol and (2) aqueous colloidal suspension of hydroxyapatite: a – electron diffraction area; b – high-resolution TEM image.

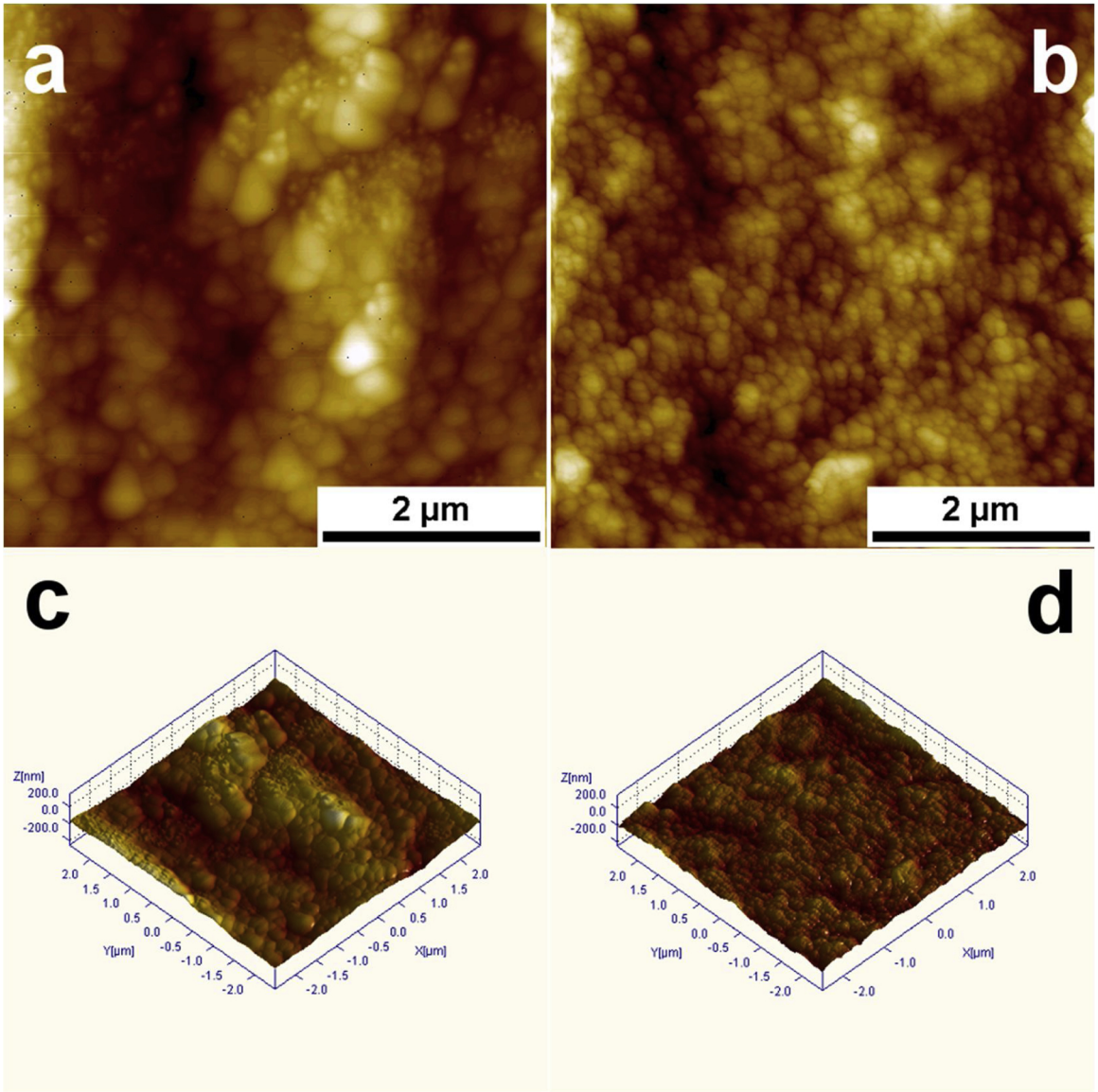

Fig. 2. (a, b) The topography and (c, d) 3D-image of tooth surface (sample 1, Table 1) before (a, c) and after (b, d) immersion in gel 1 for one month at room temperature.

Table 1
The roughness characteristics of different enamel surfaces (n = 3) before and after immersion in gel 1 for one month at room temperature.

Sample No.	Experiment	Values of roughness parameters (mean value of 5 measurements), nm				Mean values of roughness parameters at n = 3[a], nm				Decrease of the surface roughness, %			
		S_a	S_q	ΔS_a	ΔS_q	S_a	S_q	ΔS_a	ΔS_q	S_a	S_q	ΔS_a	ΔS_q
1	Before immersion	17.0	21.7	3.4	4.0	20.9	27.7	5.1	6.4	–	–	–	–
2		12.4	16.2	2.1	2.6								
3		33.3	45.2	9.8	12.7								
1	After immersion	16.1	21.1	1.9	2.3	19.5	26.5	3.3	5.1	7	4	35	20
2		11.8	15.5	1.0	1.6								
3		30.7	43.0	7.1	11.3								

S_a – arithmetical mean.
S_q – root mean square.
ΔS_a – confidence interval (Δ) of S_a.
ΔS_q – confidence interval (Δ) of S_a.
[a] The quantity of tooth enamel microsections amounted to three samples (n = 3).

and root mean square (S_q) roughness and the values of confidence intervals (ΔS_a and ΔS_q) were calculated by statistical analysis (Table 1).

It is seen that averaged values of S_a and S_q decreased noticeably after immersion in gel 1, by about 7 and 4 %, respectively. At the same time, the variation in ΔS_a and ΔS_q (about 35 and 20 %, respectively) demonstrates much greater decreasing that indicates more uniform sample surface after immersion.

To improve remineralization properties, gel 2 was synthesized, which had the HA content increased from 0.75 wt.% (gel 1) up to 1.75 wt.%, with the silicon content remaining the same (2.04 wt.%). Gel 2 as well as gel 1 has a consistency acceptable for practical use. The gel is stable at storage, when dispersed; the gel readily is converted to ointment-like state and easily spread upon injured tissues and tooth enamel surface. An increase in the HA content in the gel more than 1.75 wt.% with the silicon content remaining the same gradually results in a higher brittleness and in uneven distribution of the gel on the tooth surface, which impairs spread ability of the gel.

Fig. 3 presents the TEM image of the sample produced by drying of gel 2 suspension in ethanol on a copper grid.

As follows from Fig. 3 there are nanoscale particles in the high resolution area. Moreover the electron diffraction area confirms the crystallinity of HA in the gel.

Fig. 4 shows the typical topography (a, b) and 3D-images (c, d) of the surface relief of tooth enamel (sample 1) before and after immersion in gel 2 for one month at room temperature. The values of roughness S_a and S_q, and the value of confidence intervals ΔS_a and ΔS_q are presented in Table 2.

Comparison of the data from Table 1 and Table 2 reveals that the decreasing of averaged values of S_a and S_q for gel 2 (about 26 and 25 %, respectively), and the confidence interval ΔS_a and ΔS_q (about 57 and 58 %, respectively) are considerably greater than for gel 1.

Thus, Si-HA–glycerohydrogel containing 1.75 wt.% HA and 2.04 wt.% Si has pronounced remineralizing effect. That is, immersion of tooth enamel samples in the gel significantly reduces roughness and makes the enamel surface more uniform. As that was observed, the bioactive silicon was seen to cause an additional positive effect on enamel remineralization.

It was shown that silicon in the enamel imparts its required strength. Thus, the beaver enamel microhardness is higher than that of humans, because the chemical composition of beaver enamel has an increased content of some elements, silicon included [47].

The Vickers microhardness test and the energy dispersive X-ray analysis were performed to determine the effect of silicon on the remineralization process.

The tooth enamel samples after a one-month immersion in gel 2 (5 samples) and in model system (5 samples) were investigated by the energy dispersive X-ray analysis to determine Si, Ca, and P contents. The aqueous glycerol suspension of HA (1.75 wt.%) without silicon glycerolates was used as a model system (see the Experimental part).

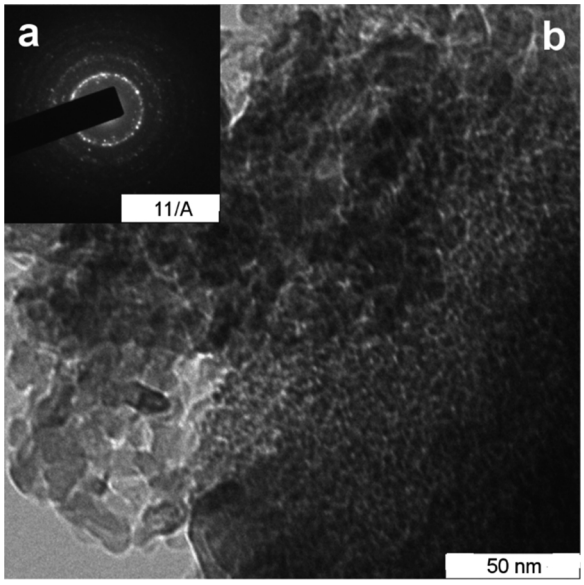

Fig. 3. TEM micrograph of dried suspension of gel 2 in ethanol: (a) electron diffraction area, (b) high-resolution TEM image.

Table 3 summarizes the results of quantitative measurements of Si, Ca, and P contents (wt.%) on the surface of tooth enamel as compared with the control samples.

Table 3 shows a statistically significant increase of the silicon content in the samples treated with gel 2 in comparison with the model system and control samples.

The microhardness indexes of tooth enamel determined by the Vickers microhardness test for the same 5 samples after treatment with gel 2 and the model system (see Table 3) are presented in Table 4.

The microhardness index of tooth enamel after treatment with gel 2 increased by 1.45 times as compared to the model system. Thus, treatment of tooth enamel samples with gel 2 improves the strength characteristics of the tooth enamel.

4. Conclusion

As a result of this study, the nanocomposite silicon-hydroxyapatite–glycerohydrogel (Si-HA–glycerohydrogel) having different hydroxyapatite (HA) contents (0.75 and 1.75 wt.%) and the same content of Si (2.04 wt.%) was obtained by the sol–gel method. Glycerol solution of silicon tetraglycerolate as a biocompatible precursor and aqueous colloid suspension of HA as a template and a property modifier

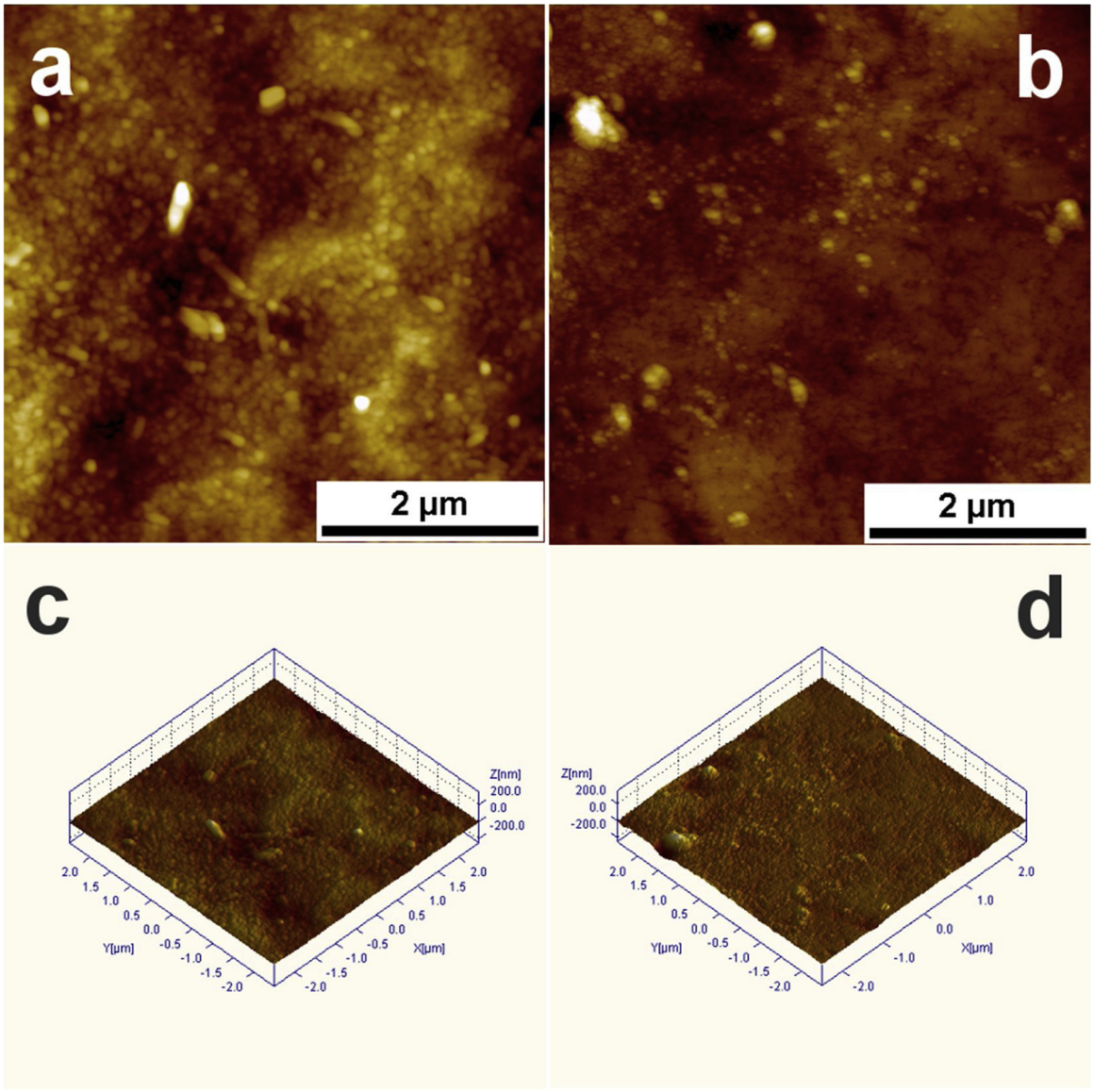

Fig. 4. (a, b) The topography and (c, d) 3D-image of tooth surface (sample 1, Table 2) before (a, c) and after (b, d) immersion in gel 2 for one month at room temperature.

were used. The transmission electron microscopy studies demonstrated that nanoscale HA Si-HA–glycerohydrogel is in the crystalline state.

For the first time, the atomic force microscopy method was applied to study the remineralizing properties of Si-HA–glycerohydrogel on human teeth extracted for orthodontic reasons. For quantitative characterization of enamel surface relief, the surface topography of enamel

Table 2
The roughness characteristics of different enamel surfaces (n = 3) before and after immersion in gel 2 for one month at room temperature.

Sample No.	Experiment	Values of roughness parameters (mean value of 5 measurements), nm				Mean values of roughness parameters at n = 3[a], nm				Decrease of the surface roughness, %			
		S_a	S_q	ΔS_a	ΔS_q	S_a	S_q	ΔS_a	ΔS_q	S_a	S_q	ΔS_a	ΔS_q
1	Before immersion	8.5	11.4	3.1	4.3	17.2	22.5	4.2	5.5	–	–	–	–
2		14.5	18.0	1.8	2.1								
3		28.7	38.1	7.8	10.0								
1	After immersion	7.2	9.5	1.1	1.4	12.8	16.8	1.8	2.3	26	25	57	58
2		13.0	16.4	1.7	2.0								
3		18.1	24.5	2.5	3.4								

S_a – arithmetical mean.
S_q – root mean square.
ΔS_a – confidence interval (Δ) of S_a.
ΔS_q – confidence interval (Δ) of S_a.
[a] The quantity of tooth enamel microsections amounted to three samples (n = 3).

Table 3
Elemental analysis (Si, Ca, P, wt.%) of tooth enamel surface layer.

Element	Tooth enamel microsections after immersion in gel 2[a]	Tooth enamel microsections after immersion in the model system[a]	Control samples[b] (without treatment)
Si	0.62 ± 0.12[c]	0.19 ± 0.04	0.16 ± 0.04
Ca	40.28 ± 5.15	38.98 ± 4.90	36.68 ± 4.35
P	22.48 ± 1.94	21.52 ± 1.62	19.98 ± 1.75

[a] The mean value obtained from analysis of 5 samples of tooth enamel.
[b] The mean value obtained from analysis of 10 samples of tooth enamel.
[c] $p \leq 0.05$, the results are statistically significant in comparison with the model system and control samples.

Table 4
The microhardness indexes of tooth enamel.

Tooth enamel microsections	Tooth enamel microhardness by Vickers (MPa)
Samples after immersion in gel 2	4160 ± 390[a]
Samples after immersion in the model system	2870 ± 280

[a] $p \leq 0.05$, the results are statistically significant.

samples kept in the gels studied for one month at room temperature was measured. The values of arithmetical mean (S_a) and root mean square (S_q) roughness and the values of confidence intervals (ΔS_a and ΔS_q) were calculated. It was found that Si-HA–glycerohydrogel containing 1.75 wt.% of HA has a pronounced remineralizing effect, namely, it reduces roughness of tooth enamel and makes enamel surface more uniform. It was demonstrated the decreasing of average values S_a and S_q (by about 26 and 25 %, respectively) and ΔS_a and ΔS_q (by about 57 and 58 %, respectively).

Silicon in a biologically active and accessible form causes an additional positive effect on the process of remineralization of tooth enamel. Using the energy dispersive X-ray analysis, it has been found that the silicon content is increased in the tooth enamel. We have demonstrated that the Vickers microhardness is also increased.

The analysis of the obtained data makes it possible to consider the Si-HA–glycerohydrogel containing 1.75 wt.% of HA as a promising biomaterial for tooth enamel remineralization. This gel can be recommended for use in dental practice, for example, as a toothpaste with reparative, regenerative and remineralizing effect.

CRediT authorship contribution statement

T.G. Khonina: Methodology. **O.N. Chupakhin:** Supervision. **V.Ya. Shur:** Investigation. **A.P. Turygin:** Investigation. **V.V. Sadovsky:** Conceptualization. **Yu.V. Mandra:** Writing - review & editing. **E.A. Sementsova:** Investigation. **A.Yu Kotikova:** Writing - original draft. **A.V. Legkikh:** Formal analysis. **E.Yu Nikitina:** Investigation. **E.A. Bogdanova:** Formal analysis. **N.A. Sabirzyanov:** Writing - original draft.

Declaration of Competing Interest

The authors declare that they have no known competing financial interests or personal relationships that could have appeared to influence the work reported in this paper.

Acknowledgments

Equipment of the Center for Joint Use “Modern Nanotechnology” (Ural Federal University) and “Spectroscopy and Analysis of Organic Compounds” (Postovsky Institute of Organic Synthesis of the Russian Academy of Sciences) was used. This work was partially carried out in the framework of State Assignment of the Russian Federation to the Institute of Solid State Chemistry of the Russian Academy of Sciences [grant No AAAA-A19-119031890028-0] and the Postovsky Institute of Organic Synthesis of the Russian Academy of Sciences [grant No AAAA-A19-119011790134-1].

Appendix A. Supplementary data

Supplementary material related to this article can be found, in the online version, at doi:https://doi.org/10.1016/j.colsurfb.2020.110851.

References

[1] L.L. Hench, Sol–gel Silica: Properties, Processing, and Technology Transfer, Noyes Publications, New Jersey, 1998, p. 168.
[2] S. Sakka, Handbook of Sol-gel Science and Technology: Applications of Sol–gel Technology, Vol. 3, Kluwer, Boston, 2005, p. 791.
[3] D. Levy, M. Zayat, The Sol-Gel Handbook. V. 1, Synthesis and Processing, Wiley – VCH Verlag GmbH & Co, Weinheim, 2015.
[4] G.J. Owens, R.K. Singh, F. Foroutan, M. Alqaysi, C.M. Han, C. Mahapatra, H.W. Kim, J.C. Knowles, Sol-gel based materials for biomedical applications, Prog. Mater. Sci. 77 (2016) 1–79, https://doi.org/10.1016/j.pmatsci.2015.12.001.
[5] K. Zheng, A.R. Boccaccini, Sol-gel processing of bioactive glass nanoparticles: a review, Adv. Colloid Interface Sci. 249 (2017) 363–373, https://doi.org/10.1016/j.cis.2017.03.008.
[6] M.A. Brook, Y. Chen, K. Guo, Z. Zhang, J.D. Brennan, Sugar-modified silanes: precursors for silica monoliths, J. Mater. Chem. 14 (2004) 1469–1479, https://doi.org/10.1039/B401278J.
[7] D. Brandhuber, V. Torma, C. Raab, H. Peterlik, A. Kulak, N. Hüsing, Glycol-modified silanes in the synthesis of mesoscopically organized silica monoliths with hierarchical porosity, Mater. Chem. 17 (2005) 4262–4271, https://doi.org/10.1021/cm048483j.
[8] Y.U.A. Shchipunov, T.Y.U. Karpenko, A.V. Krekoten, I.V. Postnova, Gelling of otherwise nongelable polysaccharides, J. Colloid Interface Sci. 287 (2005) 373–378, https://doi.org/10.1016/j.jcis.2005.02.004.
[9] T.G. Khonina, A.P. Safronov, E.V. Shadrina, M.V. Ivanenko, A.I. Suvorova, O.N. Chupakhin, Mechanism of structural networking in hydrogels based on silicon and titanium glycerolates, J. Colloid Interface Sci. 365 (2012) 81–89, https://doi.org/10.1016/j.jcis.2011.09.018.
[10] T.G. Khonina, A.P. Safronov, M.V. Ivanenko, E.V. Shadrina, O.N. Chupakhin, Features of silicon– and titanium–polyethylene glycol precursors in sol–gel synthesis of new hydrogels, J. Mater. Chem. B Mater. Biol. Med. 3 (2015) 5490–5500, https://doi.org/10.1039/C5TB00480B.
[11] E.A. Bogdanova, N.A. Sabirzyanov, T.G. Khonina, Hydroxyapathite gel as a basis for pharmaceutic composites, Glass Phys. Chem. 37 (2011) 533–536, https://doi.org/10.1134/S1087659611050038.
[12] T.G. Khonina, O.N. Chupakhin, L.P. Larionov, T.G. Boyakovskaya, A.L. Suvorov, E.V. Shadrina, Synthesis, toxicity, and percutaneous activity of silicon glycerolates and related hydrogels, Pharm. Chem. J. 42 (2008) 609–613, https://doi.org/10.1007/s11094-009-0199-x.
[13] N.A. Sabirzjanov, E.A. Bogdanova, T.G. Khonina, Method of Preparing Hydroxyapatite Suspension, (2010) RU2406693.
[14] F.H. Nielsen, Update on the possible nutritional importance of silicon, J. Trace Elem. Med. Biol. 28 (4) (2014) 379–382, https://doi.org/10.1016/j.jtemb.2014.06.024.
[15] N. Roveri, E. Foresti, M. Lelli, I.G. Lesci, M. Marchetti, Microscopic investigations of synthetic biomimetic hydroxyapatite, in: A. Méndez-Vilas, J. Díaz (Eds.), Microscopy: Science, Technology, Applications and Education, V. 3, Formatex, Badajoz, 2010, pp. 1868–1879.
[16] H. Zhou, J. Lee, Nanoscale hydroxyapatite particles for bone tissue engineering, Acta Biomater. 7 (2011) 2769–2781, https://doi.org/10.1016/j.actbio.2011.03.019.
[17] S. Mazumder, A.K. Nayak, T.J. Ara, M.S. Hasnain, Hydroxyapatite composites for dentistry, in: A.M. Asiri, D. Inamuddin, A. Mohammad (Eds.), Applications of Nanocomposite Materials in Dentistry, Woodhead Publishing, Duxford, 2019, pp. 123–143.
[18] K. Fox, P.A. Tran, N. Tran, Recent advances in research applications of nanophase hydroxyapatite, ChemPhysChem. 13 (2012) 2495–2506, https://doi.org/10.1002/cphc.201200080.
[19] J. Venkatesan, S.K. Kim, Nano-hydroxyapatite composite biomaterials for bone tissue engineering – a review, J. Biomed. Nanotechnol. 10 (2014) 3124–3140, https://doi.org/10.1166/jbn.2014.1893.
[20] C. Ding, Z. Chen, J. Li, From molecules to macrostructures: recent development of bioinspired hard tissue repair, Biomater. Sci. 5 (2017) 1435–1449, https://doi.org/10.1039/C7BM00247E.
[21] N. Juntavee, A. Juntavee, P. Plongniras, Remineralization potential of nano-hydroxyapatite on enamel and cementum surrounding margin of computer-aided design and computer-aided manufacturing ceramic restoration, Int. J. Nanomedicine 13 (2018) 2755–2765, https://doi.org/10.2147/IJN.S165080.
[22] K. Lin, C. Wu, J. Chang, Advances in synthesis of calcium phosphate crystals with

controlled size and shape, Acta Biomater. 10 (2014) 4071–4102, https://doi.org/10.1016/j.actbio.2014.06.017.
[23] A. Szcześ, L. Hołysz, E. Chibowski, Synthesis of hydroxyapatite for biomedical applications, Adv. Colloid Interface Sci. 249 (2017) 321–330, https://doi.org/10.1016/j.cis.2017.04.007.
[24] P. Terzioğlu, H. Öğüt, A. Kalemtaş, Natural calcium phosphates from fish bones and their potential biomedical applications, Mater. Sci. Eng. C. 91 (2018) 899–911, https://doi.org/10.1016/j.msec.2018.06.010.
[25] Z. Zhuang, H. Yoshimura, M. Aizawa, Synthesis and ultrastructure of plate-like apatite single crystals as a model for tooth enamel, Mater. Sci. Eng. C. 33 (2013) 2534–2540, https://doi.org/10.1016/j.msec.2013.02.035.
[26] X. Zhang, X. Deng, Y. Wu, Remineralizing nanomaterials for minimally invasive dentistry, in: A. Kishen (Ed.), Nanotechnology in Endodontics: Current and Potential Clinical Applications, Springer, New York, 2015, pp. 173–193, , https://doi.org/10.1007/978-3-319-13575-5.
[27] E. Abou Neel, A. Aljabo, A. Strange, S. Ibrahim, M. Coathup, A. Young, L. Bozec, V. Mudera, Demineralization–remineralization dynamics in teeth and bone, Int. J. Nanomedicine 11 (2016) 4743–4763, https://doi.org/10.2147/IJN.S107624.
[28] L. Li, H. Pan, J. Tao, X. Xu, C. Mao, X. Gu, R. Tang, Repair of enamel by using hydroxyapatite nanoparticles as the building blocks, J. Mater. Chem. 18 (2008) 4079–4084, https://doi.org/10.1039/B806090H.
[29] A. Mielczarek, J. Michalik, The effect of nano-hydroxyapatite toothpaste on enamel surface remineralization. An in vitro study, Am. J. Dent. 27 (2014) 287–290.
[30] N. Philip, State of the art enamel remineralization systems: the next frontier in caries management, Caries Res. 53 (2019) 284–295, https://doi.org/10.1159/000493031.
[31] M. Vano, G. Derchi, A. Barone, U. Covani, Effectiveness of nano-hydroxyapatite toothpaste in reducing dentin hypersensitivity: a double-blind randomized controlled trial, Quintessence Int. (Berl) 45 (8) (2014) 703–711, https://doi.org/10.3290/j.qi.a32240.
[32] D. Pei, Y. Meng, Y. Li, J. Liu, Y. Lu, J. Mech, Influence of nano-hydroxyapatite containing desensitizing toothpastes on the sealing ability of dentinal tubules and bonding performance of self-etch adhesive, Behav. Biomed. Mater. 91 (2019) 38–44, https://doi.org/10.1016/j.jmbbm.2018.11.021.
[33] N.A. Sabirzjanov, L.P. Larionov, S.P. Jatsenko, T.G. Bojakovskaja, Method for Producing Wound-healing and Osteoplastic Means, (2008) RU2314107.
[34] E. Landi, S. Sprio, M. Sandri, A. Tampieri, L. Bertinetti, G. Martra, Development of multisubstituted apatites for bone reconstruction, Key Eng. Mater. 361 (2007) 171–174, https://doi.org/10.4028/www.scientific.net/KEM.361-363.171.
[35] Z. Dong, J. Chang, Y. Zhou, K. Lin, In vitro remineralization of human dental enamel by bioactive glasses, J. Mater. Sci. 46 (2011) 1591–1596, https://doi.org/10.1007/s10853-010-4968-4.
[36] L. Han, T. Okiji, Bioactivity evaluation of three calcium silicate-based endodontic materials, Int. Endod. J. 46 (2013) 808–814, https://doi.org/10.1111/iej.12062.
[37] S. Pilch, D. Masters, Composition for Teeth Care and Method of Treatment and Prevention of Damage to Tooth Surface, (2014) RU2517332.
[38] R.A. Bapat Chaitanya, P. Joshi Prachi, Bapat Tanay, V. Chaubal, R. Pandurangappa, N. Jnanendrappa, B. Gorain, S. Khurana, P. Kesharwani, The use of nanoparticles as biomaterials in dentistry, Drug Discov. Today 24 (1) (2019) 85–98, https://doi.org/10.1016/j.drudis.2018.08.012.
[39] B.R. Ware, W.H. Flygare, Light scattering in mixtures of BSA, BSA dimers, and fibrinogen under the influence of electric fields, J. Colloid Interface Sci. 39 (1972) 670–675, https://doi.org/10.1016/0021-9797(72)90075-6.
[40] W.W. Tscharnuter, R.A. Meyers (Ed.), Encyclopedia of Analytical Chemistry, Wiley, New York, 2001, , https://doi.org/10.1021/ed082p1313.2.
[41] F. Lippert, D.M. Parker, K.D. Jandt, In vitro demineralization/remineralization cycles at human tooth enamel surfaces investigated by AFM and nanoindentation, J. Colloid Interface Sci. 280 (2004) 442–448, https://doi.org/10.1016/j.jcis.2004.08.016.
[42] U. Maver, T. Velnar, M. Gaberšček, O. Planinšek, M. Finšgar, Recent progressive use of atomic force microscopy in biomedical application, Trends Analyt. Chem. 80 (2016) 96–111, https://doi.org/10.1016/j.trac.2016.03.014.
[43] X. Li, D. Pan, S. Lin, Z. Zhuang, Z. Lin, Facile in vitro hydroxyapatite remineralization of human enamel with remarkable hardness, CrystEngComm. 15 (2013) 4351–4356, https://doi.org/10.1039/C3CE26947G.
[44] M. Lombardini, M. Ceci, M. Colombo, S. Bianchi, C. Poggio, Preventive effect of different toothpastes on enamel erosion: AFM and SEM studies, Scanning 36 (2014) 401–410, https://doi.org/10.1002/sca.21132.
[45] B.-D. Lechner, S. Röper, J. Messerschmidt, A. Blume, R. Magerle, Monitoring demineralization and subsequent remineralization of human teeth at the dentin–Enamel junction with atomic force microscopy, ACS appl. Mater. Interfaces 7 (34) (2015) 18937–18943, https://doi.org/10.1021/acsami.5b04790.
[46] Y. Wang, L. Mei, L. Gong, J. Li, S. He, Y. Ji, W. Sun, Remineralization of early enamel caries lesions using different bioactive elements containing toothpastes: an in vitro study, Technol. Health Care 24 (2016) 701–711, https://doi.org/10.3233/THC-161221.
[47] A.A. Kunin, A.Y. Evdokimova, N.S. Moiseeva, Age-related differences of tooth enamel morphochemistry in health and dental caries, EPMA J. 6 (2015) 3, https://doi.org/10.1186/s13167-014-0025-8.